ANALYSIS OF EDDY CURRENT DISTRIBUTION AND RESULTING FLAW DETECTION MECHANISM FOR SELF-NULLING PROBE

Buzz Wincheski, Jim Fulton, and Shridhar Nath
Analytical Services and Materials
107 Research Drive
Hampton, VA 23666

Min Namkung
NASA Langley Research Center
MS 231
Hampton, VA 23681

INTRODUCTION

The Self-Nulling Probe developed at NASA-LaRC has been previously shown to simplify inspections and increase detectability of surface and subsurface flaws in conductive materials [1]. The operation of the probe has been explained in terms of a redistribution of the eddy currents and associated magnetic field by the presence of inhomogeneities in the test article [1, 2]. In the present work a mathematical model is introduced to calculate the eddy current flow induced by the Self-Nulling Probe in test samples containing through notch flaws. The model combines axisymmetric finite element modeling (FEM) with conformal mapping techniques in order to calculate the stream function of the induced current flow about arbitrarily sized and positioned notches. Physical parameters such as the induced eddy current density, magnetic field normal to the surface of the sample, and probe output voltage are then calculated from the stream function of the induced current flow. Simulation results are compared with experimental measurements taken on calibration standards with good agreement.

FINITE ELEMENT MODELING RESULTS

The solution for the magnetic field and eddy current distribution of the Self-Nulling Probe operating on unflawed material has been previously solved by the finite element approach [1]. In these models the symmetry of the probe and sample were used in order to reduce the geometry to a two dimensional problem. Fig. 1 displays the results of axisymmetric FEM of the self nulling probe over unflawed material. The displayed results are for an operating frequency of 70 kHz.

The solution for the field quantities when the probe is operated over a sample containing a fatigue crack is a much more difficult problem. The presence of the flaw destroys the

Review of Progress in Quantitative Nondestructive Evaluation, Vol. 14
Edited by D.O. Thompson and D.E. Chimenti, Plenum Press, New York, 1995

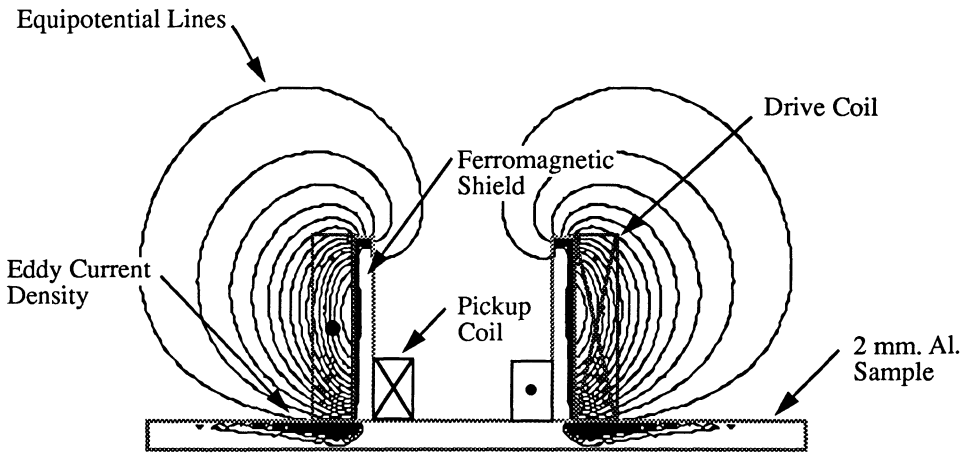

Fig. 1. Axisymmetric finite element results for eddy current density and equipotential contours about probe operating above unflawed sample.

symmetry of the problem so that two dimensional FEM can no longer be applied. The complexity in moving to a three dimensional code can become overwhelming, with huge increases in computer memory and solution times required [3]. In addition, the calculation of the output signal of the self-nulling probe requires an accurate solution for the fields passing around the ferromagnetic shield. The electromagnetic energy in this region is by design much lower than that in the neighboring areas, making an accurate calculation of the probe output even more difficult.

CONFORMAL MAPPING OF EDDY CURRENT STREAM FUNCTION

As an alternative approach to three dimensional FEM, a hybrid finite element/conformal mapping approach has been developed to solve for the probe output over through notch flaws. FEM is used to solve the electromagnetic problem in the symmetric case when no flaw is present in the sample. The flow problem of the current distribution about flaws is then solved through conformal mapping techniques.

Electromagnetic phenomena are governed by the continuity equation for charge conservation;

$$\frac{\partial \rho}{\partial t} + \nabla \cdot \bar{J} = 0, \qquad (1)$$

where ρ and $\bar{J}$ are the charge and current densities respectively [4]. For steady state magnetic phenomena there is no change is the net charge density anywhere in space; $\partial\rho/\partial t = 0$. The simplified continuity equation for harmonic eddy current flow is therefore

$$\nabla \cdot \bar{J} = 0. \qquad (2)$$

The Lagrangian stream function ψ, defined for plane two dimensional flows by the relations

$$J_x = \frac{\partial \psi}{\partial y}, \qquad J_y = -\frac{\partial \psi}{\partial x}, \qquad (3)$$

can now be introduced as a scalar function which determines $\bar{J}$. Using (3) the continuity equation (2) can be written in terms of the stream function as

$$\frac{\partial^2 \psi}{\partial x \partial y} - \frac{\partial^2 \psi}{\partial y \partial x} = 0. \qquad (4)$$

This equation will be valid for any smoothly varying function ψ. A solution obtained for the

eddy current distribution using the Lagrangian stream function as defined in (3) will therefore be valid as long as the function ψ is well behaved.

The direction and magnitude of the induced eddy current flow can be visualized by looking at a plot of constant ψ lines. The lines of constant ψ are known as streamlines of the flow, with the direction of the current flow being along the streamlines and the current density being inversely proportional to the spacing between adjacent lines [5]. Fig. 2 shows a sketch of the streamlines of the induced eddy current flow in both an unflawed sample and a sample containing a through EDM notch. The inner dashed circle in the sketches represents the outer diameter of the pickup coil of the probe. The presence of the EDM notch, drawn as a dashed line in fig. 2b, will force the otherwise circular eddy currents to flow about the tips of the notch. In the present work only notches which penetrate through the thickness of the sample are considered. This constraint simplifies the problem by prohibiting current flow under the notch, thereby allowing two dimensional conformal mapping techniques to be applied.

The unflawed eddy current stream function can be directly calculated from axisymmetric FEM. The FEM results will provide a solution for the vector potential, A. The eddy current density at each point is then

$$\bar{J} = J_\theta = \sigma\omega A_\theta \tag{5}$$

where σ is the conductivity and ω is the circular frequency. The definition for ψ in plane polar coordinates corresponding to (3) is

$$rJ_r = \frac{\partial\psi}{\partial\theta}, \qquad J_\theta = -\frac{\partial\psi}{\partial r}. \tag{6}$$

Substituting (5) into (6) and solving for ψ yields

$$\psi(r, \theta) = \omega\int_0^r \sigma A_\theta dr. \tag{7}$$

Once the unflawed steam function is determined from (7) conformal mapping techniques can be used to calculate the flow pattern in regions containing arbitrarily sized and shaped notches. The unknown solution is obtained by transforming the geometry for the unflawed flow into the flawed geometry where a notch is present. The transformation functions which accomplish this mapping are then applied to the unflawed stream function (7) to give the stream function of the current flow in the presence of notch type defects.

The three dimensional problem of determining the induced eddy current flow in a sample containing a through EDM notch is then solved by transforming the stream function of the eddy current flow of fig. 2a. until the geometry matches that of fig. 2b. This transformation process is accomplished with the use of complex transformation functions which

Fig. 2. Streamlines of eddy current flow for unflawed sample (a) and sample containing a through EDM notch (b).

provide a one to one mapping between points in the complex plane while maintaining the magnitude and sense of angles between curves in the plane. Tables of transformations between regions in the complex plane and the associated complex mapping functions are available in the literature [6]. The required transformations for mapping region 2a into region 2b are illustrated in fig. 3. Once again, the inner dashed circle represents the pickup coil location and the EDM notch is drawn as a dashed line segment.

Fig. 3a shows the unflawed flow pattern drawn in the Z=x+iy plane. Figs. 3b-h are the intermediate planes used to arrive at the plane of the flow pattern to be solved, illustrated in fig. 3i. The complex mapping function between any two consecutive planes is written

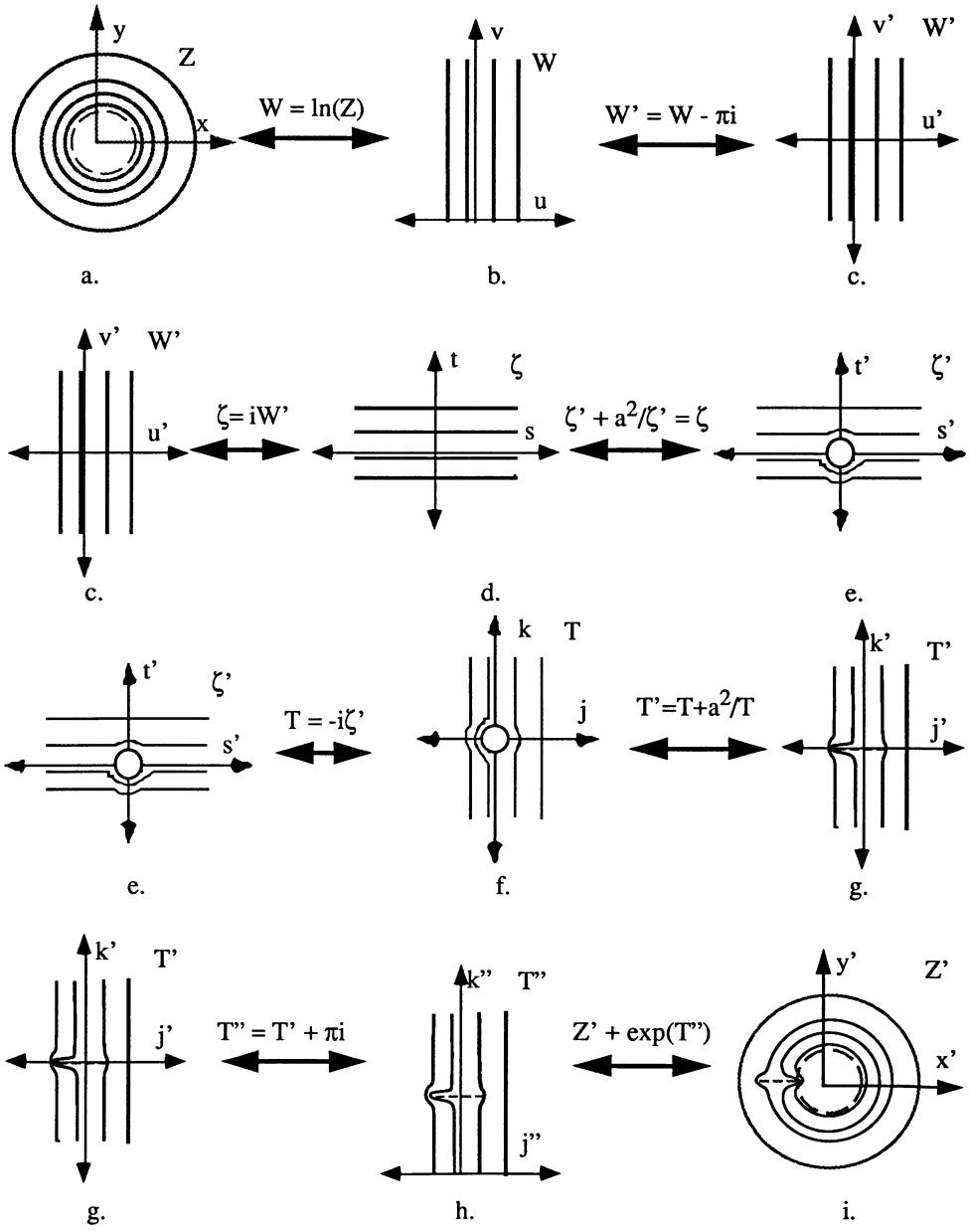

Fig. 3. Conformal mapping of unflawed eddy current flow into flow about EDM notch.

between the planes it connects.

The transformation process begins with the logarithmic function which maps a circle of unit radius centered about the origin into the imaginary axis between 0 and $2\pi i$, as shown in figs. 3a-b. The flow pattern is then translated so that it is centered about the real axis as seen in fig. 3c. At this point the flow pattern is rotated and the Joukowsky transformation is applied. The Joukowsky transformation opens the line segment from $-2a$ to $2a$ along the real axis into a circle of radius a centered at the origin [5]. The flow about the cylindrical obstacle is then rotated back to the vertical direction and the inverse Joukowsky transformation is applied in order to squash the cylindrical obstacle into a line segment perpendicular to the flow, as depicted in fig 3g. Next, the region is translated to the plane drawn in fig. 3h. Finally, the exponential transformation is used to wrap the geometry to the region of the flawed eddy current flow of fig. 3i. Solutions for arbitrarily sized flaws can be generated by changing the value of the variable a in the Joukowsky transformation, while changes to the position of the flaw require extra transformations to translate the flow which are not shown in the figure.

Once the complex mapping functions between the planes 3a and 3i are determined the stream function about the EDM notch can be calculated by applying the transformations to the stream function for the flow in an unflawed sample as determined through axisymmetric finite element modeling. The eddy current distribution about the flaw is then determined from equation (6).

In the calculations performed for the present work, the unflawed stream function of fig. 3i has been approximated as

$$\psi = \mathrm{erf}(1.5\ln(x'^2 + y'^2)) . \qquad (8)$$

It was found that this function gives good qualitative agreement with FEM results for the unflawed flow. The use of equation (8) guarantees the smoothness of ψ which, in turn, guarantees that the final solution for the eddy current distribution will satisfy the continuity equation (2), as explained above. The application of the transformation functions illustrated in fig. 3 are also greatly simplified through the use of the single functional dependence of ψ on position.

RESULTS

Fig. 4 shows the calculated streamlines for four different flaw configurations. In fig. 4a the streamlines for the unflawed flow of equation (8) are drawn. This flow pattern corresponds to figs. 2a and 3a. Figs. 4b and 4c display the distortion to the eddy current flow caused by an EDM notch equal in length to the diameter of the probe, where the probe diameter is defined as the inside diameter of the ferromagnetic shield. The notch tip position has been changed between the figures in order to illustrate the effect of moving the probe toward a flaw. In fig. 4d the streamlines for a notch equal in length to the radius of the probe are shown. The streamline plots provide a detailed picture of the induced eddy current flow and thereby can yield significant insight into the operating characteristics of the probe. The bunching of the streamlines at the notch tips, indicating an increased current density, is evident in figs. 4c and 4d. In addition, the shifting of the inner streamlines to a position directly under the pickup coil can be seen in figs. 4b-4d. This indicates that part of the eddy current distribution is now located directly under the pickup coil. The magnetic induction associated with this current flow will therefore link with the pickup and induce a voltage across the pickup leads.

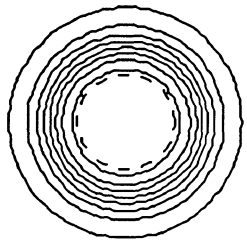

a. Unflawed Sample

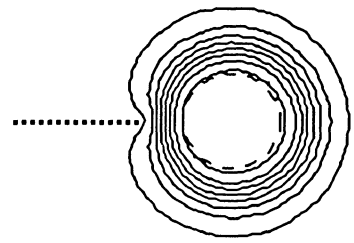

b. Notch length = Probe diameter
Notch tip = 1.375 * Probe Radius

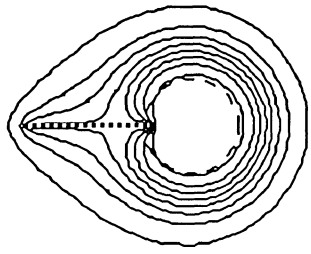

c. Notch length = Probe diameter
Notch tip = Probe Radius

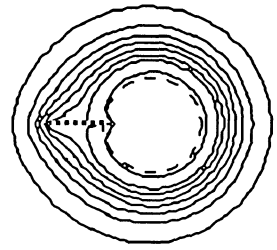

d. Notch length = Probe Radius
Notch tip = Probe Radius

Fig. 4. Calculated streamlines for various notch positions.

In order to compare simulation results with measurements on calibration standards and to predict the operating characteristics of experimental probe designs, physical quantities must be extracted from the streamfunction. The eddy current flow can be directly calculated from ψ through the use of equation (6). The magnetic induction normal to the pickup coil cross section is determined from

$$\nabla \times \bar{E} = -\frac{1}{c}\frac{\partial \bar{B}}{\partial t}. \tag{9}$$

Since

$$\bar{B} = \nabla \times \bar{A}, \tag{10}$$

equation (9) reduces to

$$\bar{E} = -\frac{1}{c}\frac{\partial \bar{A}}{\partial t}. \tag{11}$$

Now, at the surface of the conductor

$$\bar{J} = \sigma \bar{E}, \tag{12}$$

so that, substituting in the value of $\bar{E}$ from equation (11),

$$\bar{J} = \frac{\sigma}{c}\frac{\partial \bar{A}}{\partial t}. \tag{13}$$

For steady state fields

$$\bar{A} = \bar{A}_0 e^{j\omega t}, \tag{14}$$

yielding

$$\bar{J} = -\frac{\sigma j\omega}{c}\bar{A}_0 \tag{15}$$

or

$$\bar{A}_0 = -\frac{c}{\sigma j\omega}\bar{J}. \tag{16}$$

Substituting this value for the vector potential back into equation (10) gives the solution for the magnetic induction at the surface of the sample;

$$\bar{B} = -\frac{c}{\sigma j\omega}(\nabla \times \bar{J}). \tag{17}$$

The magnitude of the B field normal to the pickup coil windings is then, for the sample in the x,y plane,

$$|B_z| \propto (\nabla \times \bar{J})_z = \frac{\partial J_y}{\partial x} - \frac{\partial J_x}{\partial y}. \tag{18}$$

Since the normal B field is continuous across an interface, B_z just inside the conductor will be equal to the field just above the sample surface. Fig. 5 is a plot of B_z for the streamfunctions of figs. 4a and 4c. The presence of the EDM notch is seen to increase the magnetic flux inside the dashed circle representing the location of the pickup coil. There will therefore be a significant flux linkage with the pickup coil and an induced output voltage will be detected.

The output voltage of the probe can be estimated by assuming that the number of turns cut by a magnetic flux line is proportional to the square of the difference between the radius of the pickup coil and the location of the flux line at the sample surface,

$$N \propto (r_{puc} - r')^2. \tag{19}$$

The induced voltage across the pickup coil leads can then be found from

$$V = \omega \int_{puc} NB_z da. \tag{21}$$

Equation (21) allows for simulation results to be directly compared to experimental measurements on calibration samples. Fig. 6a is a comparison between experimental and simulation results for the probe output as a function of notch length. Fig. 6b compares the simulation and experimental results for the output voltage as the probe is scanned over an EDM notch of length = 0.625(probe diameter). The plot shows the probe output as a function of the distance between the center of the probe and the center of the flaw. Since the notch length is smaller than the probe diameter, the output voltage goes to background levels when the probe is centered over the flaw. The method used to obtain the experimental data has been previously reported and so will not be discussed here [1]. The simulation results are seen to agree well with the experimental measurements in both sets of data. The small discrepancy between the simulation and experimental results for fig. 6b can be attrib-

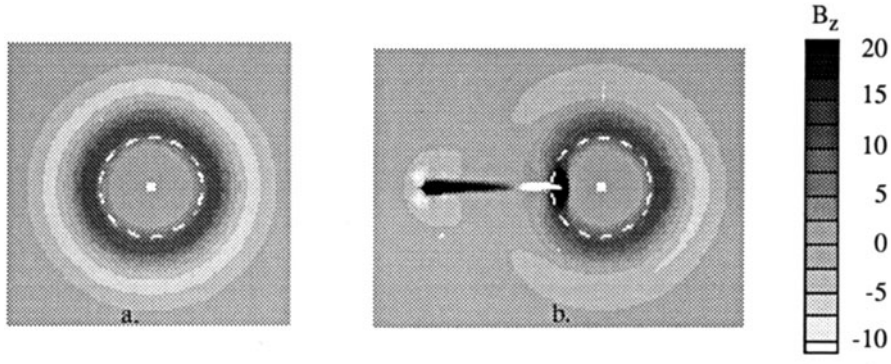

Fig. 5 Calculated magnetic induction normal to the pickup coil windings at the surface of the sample. The plots correspond to the streamfunctions of figs. 4a and 4c.

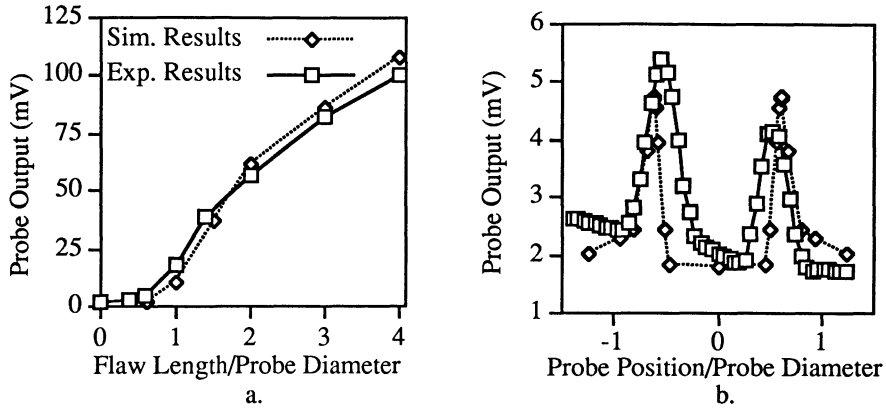

Fig. 6 Comparison of simulation results with experimental measurements on calibration standards.

uted to the errors associated with approximating the unflawed streamfunction by an error function distribution as given in equation (8). A better approximation of the unflawed flow, such as by fitting the finite element data with cubic splines, is expected to bring the simulation results into even closer agreement with experimental measurements.

SUMMARY

A hybrid finite element/conformal mapping technique has been introduced to solve for the flaw signal of the Self-Nulling Probe due to through EDM notch type flaws. The technique provides a detailed picture of the current flow, which adds significant insight into the probe operation. Calculated probe responses have been shown to agree well with experimental measurements. As the simulation results can be generated quickly without the need for large amounts of computer memory, the technique provides a mechanism for efficiently simulating flaw signals from experimental probe designs. The technique has thus far been developed only for through EDM notches which generate eddy current distributions similar to that shown in fig. 2b. The transformation functions introduced in fig. 3 will not account for induced currents which travel under the flaw, are split into two closed loop patterns, or pass directly under the center of the probe, (x', y') = (0, 0) in fig. 3i. Future research will explore methods to expand the procedure to a more general class of flaws.

REFERENCES

1. B. Wincheski, J.P. Fulton, S. Nath, N. Namkung, and J.W. Simpson, "Self-Nulling Eddy Current Probe for Surface and Subsurface Flaw Detection", in *Materials Evaluation*, Vol. 52/Number 1 (January 1994).
2. M. Namkung, C.G. Clendenin, J.P. Fulton, and B. Wincheski, *Review of Progress in QNDE,* Vol. 13B, 1633, Plenum Press, New York, 1994.
3. S. Ratnajeevan H. Hoole, *Computer-Aided Analysis and Design of Electromagnetic Devices,* 395, Elsevier Science Publishing Co., New York, 1989.
4. J.D. Jackson, *Classical Electrodynamics,* John Wiley & Sons, New York, 1975.
5. James M. Robertson, *Hydrodynamics in Theory and Practice*, Prentice-Hall Inc., Englewood Cliffs, N.J., 1965.
6. R.V. Churchill and J.W. Brown, *Complex Variables and Applications,* McGraw-Hill Publishing Company, New York, 1990.